Electronic structure of cubic $SrHfO_3$: Ferroelectric stability and detailed comparison with $SrTiO_3$

G. Fabricius
Departamento de Física, Universidad Nacional de La Plata, Calle 47 y 115, 1900 La Plata, Argentina

E. L. Peltzer y Blanca and C. O. Rodriguez
Instituto de Física de Liquidos y Sistemas Biológicos, Grupo Física del Sólido, Casilla de Correo 565, La Plata 1900, Argentina

A. P. Ayala, P. de la Presa, and A. Lopez García
Departamento de Física, Universidad Nacional de La Plata, Calle 47 y 115, 1900 La Plata, Argentina
(Received 27 August 1996)

Electronic structure calculations of cubic $SrTiO_3$ and $SrHfO_3$ are presented. The full-potential linear augmented-plane-wave method is used and exchange-correlation effects are treated by the local-density approximation. The tendency to ferroelectricity of both compounds is explored and compared by displacing the transition metal atom (Ti or Hf) towards one of the oxygens (001 direction). The calculations show that ferroelectricity is favored in $SrTiO_3$ with respect to $SrHfO_3$ and that this fact may be correlated with the degree of hybridization between transition metal d-O p bands as has been found for other related systems. Also a detailed discussion of the calculated electric field gradients is presented. [S0163-1829(97)03201-3]

INTRODUCTION

The ABO_3 compounds exhibit a variety of interesting properties which are dependent on which particular A and B elements are forming them. In particular, we are interested in those where A is an alkaline earth (Ca, Sr, or Ba) and B is a tetravalent metal (Hf or Ti). Usually they form cubic, tetragonal, orthorhombic, or rhombohedral lattices and exhibit a rich phase diagram. Anions form a regular octahedron in the cubic symmetry surrounding B atoms or distorted octahedrons in crystals with lower symmetries. It is basically this B-metal–oxygen octahedra complex that determines the different characteristics of these compounds, resulting in distinct electron distributions associated with the B-metal–oxygen covalent bonds. These systems have been extensively studied because of their possible technological applications, such as ferroelectricity, but there is also interest in the understanding of the physics underlying their phase transitions. In this work we have concentrated on a parallel study of the electronic structure of $SrTiO_3$ and $SrHfO_3$.

Although $SrHfO_3$ is a compound that has been well known for a long time, still there is no consensus about its crystalline structure. A cubic structure was determined by Hoffman[1] using x-ray diffraction with $a=4.069$ Å at room temperature. Andrade *et al.* studied $SrHfO_3$ by perturbed angular correlation spectroscopy (PAC) and determined only the strongest component of the electric field gradient (EFG) tensor to be 2.32×10^{17} V/cm^2 at ^{181}Ta probes measured at Hf sites.[2] The presence of an EFG suggests a noncubic structure. More recently, Cuffini *et al.*[3] have determined by x-ray diffraction that $SrHfO_3$ is cubic at high temperatures, but suffers a phase transition arround 600 °C to an orthorhombic structure. At the lowest temperature where the cubic phase is well defined (700 °C), the lattice parameter was found to be 4.117 Å. For the samples in the orthorhombic phase, de la Presa *et al.* obtained by PAC a value of 2.02×10^{17} V/cm^2 for the EFG at ^{181}Ta probes at room temperature.[4]

$SrTiO_3$ has the simple cubic perovskite structure at high temperature, suffers an antiferrodistortive transition at 105 K, and goes to a tetragonal phase in which the oxygen octahedra have rotated in opposite senses in neighboring unit cells. In the range 50–100 K, there is a softening of the ferroelectric (FE) polar phonons that appears to extrapolate to a FE transition close to 20 K. It is believed that quantum fluctuations supress long-range ferroelectric order at low temperatures since no FE transition is observed.[5] $SrTiO_3$ is therefore referred to as an incipient ferroelectric.

In the present work we study the electronic structure of $SrTiO_3$ and $SrHfO_3$ in the cubic phase. To our knowledge no other study of the electronic structure of $SrHfO_3$ exists in the literature, and so our first-principles study represents an important contribution. Other first-principles calculations[6,7] exist for $SrTiO_3$, but our comparative study between the two perovskites will serve to give a deeper understanding of underlying physics. We also study the tendency of $SrTiO_3$ and $SrHfO_3$ to suffer a FE transition when the B atom is displaced in the 001 direction and discuss the EFG that appears at the A and B sites when such a distorsion from the cubic symmetry is performed. This pattern for the atom distortions is not the actual ferroelectric mode, which will most probably involve not only z-axis displacements of the B cation, but will include the oxygens and A cations as well [as, for example, in the case of $KTaO_3$ (Ref. 8)]. Anyhow, a qualitative sensing of possible instabilities will be reflected by this restricted pattern movement. We find in the case of $SrTiO_3$ a clear tendency to ferroelectricity which is not present in $SrHfO_3$. Our calculations support the idea that the tendency to ferroelectricity is more important for perovskites that have a greater hybridization between B-d and O-p bands as other authors have suggested for related systems.[9] Our present cal-

culations will serve as a basis for future studies of the exact displacement pattern of the ferroelectric mode of $SrHfO_3$ and its relation to the most stable phase at low temperatures.

APPROACH

The calculations presented in this work were performed within the local density approximation (LDA) to density functional theory, using the full-potential (FP) linear augmented-plane-wave (LAPW) method.[10] In this method no shape approximation on either the potential or the electronic charge density is made. We use the WIEN95 implementation of the method,[11] which allows the inclusion of local orbitals (LO's) in the basis, improving upon linearization and making possible a consistent treatment of semicore and valence states in one energy window, hence ensuring proper orthogonality.[12] The Hedin-Lundqvist parametrization for the exchange-correlation potential is used.[13]

The atomic sphere radii (R_i) 2.5, 1.65, 1.7, and 1.78 a.u. were used for Sr, O, Ti, and Hf, respectively, in $SrTiO_3$ and $SrHfO_3$ calculations. We take for the parameter RK_{max}, which controls the size of the basis sets in these calculations, the value of 8 for both systems studied. This gives well-converged basis sets consisting of approximately 739 and 895 LAPW functions plus local orbitals for $SrTiO_3$ and $SrHfO_3$, respectively. The correctness of the choice of these parameters was checked by performing calculations for other R_i ($R_{Hf}=2$ a.u., $R_{Ti}=1.9$ a.u., and $R_{Sr}=2$ a.u.) and with increased values of RK_{max}. Even when changes in RK_{max} from 8 to 9 give no significant differences for most of physical properties we studied (bulk modulus, EFG, partial charges), to obtain a well-converged absolute value of total energy it is necessary to increase further RK_{max}. For example, to obtain a precision of 1 mRy in the cohesive energy it is necessary to take $RK_{max}=10$ for our choice of R_i. We introduce LO's to include the following orbitals in the basis set: Ti 3*s* and 3*p*, Hf 5*s* and 5*p*, Sr 4*s* and 4*p*, and O 2*s*.

Integrations in reciprocal space were performed using the special points method. We used $7\times7\times7$ meshes which represent 400 *k* points in the first Brillouin zone. In the case of displacement of the *B* ion in the (001) direction where the cubic symmetry is broken, we used less dense meshes of $5\times5\times5$, which made our calculations less expensive, still giving the precision required.

RESULTS AND DISCUSSION

We first performed calculations for $SrTiO_3$ and $SrHfO_3$ in the cubic perovskite structure as a function of the lattice parameter. Evaluating the energy as a function of volume, we obtain the theoretical value of the lattice parameter in the cubic structure and the corresponding bulk modulus. These quantities and the cohesive energy are shown in Table I and compared with available experimental values. For $SrTiO_3$ we obtain a lattice parameter which is 1% smaller than the experimental value as usually occurs in LDA calculations. The bulk modulus is also in good agreement with experimental determinations as well as with other LDA *ab initio* calculations.[15] In brackets is the bulk modulus obtained at the experimental lattice parameter, normally quoted as a more reliable evaluation from a LDA calculation. For

TABLE I. Lattice parameter (in a.u.), bulk modulus (in GPa) and cohesive energy (in Ry/cell) obtained in the present calculation and compared with available experimental results. In brackets is the bulk modulus at the experimental equilibrium volume.

		FPLAPW	Experiment
$SrTiO_3$	a	7.30	7.38[a]
	B	203(165)	174–183[a]
	E_{coh}	3.17	
$SrHfO_3$	a	7.69	7.69[b]
	B	184	
	E_{coh}	2.98	

[a]Reference 14.
[b]Reference 1.

$SrHfO_3$ our value of the lattice parameter coincides with the one obtained experimentally by Hoffman at room temperature and is approximately 1% smaller than that obtained by Cuffini *et al.* for the cubic phase at 700 °C.[3] Anyhow, recent experimental evidence seems to point out that the most stable phase at room temperature is not the cubic one, but one of orthorhombic symmetry.[3] This suggests that the previous experimental value at room temperature taken as corresponding to a cubic phase may be in fact an averaged lattice parameter from the orthorhombic one.

In Fig. 1 we show the band structure for $SrTiO_3$ and $SrHfO_3$ at our predicted values of lattice parameters. The valence band structures of both systems are very similar: They consist essentially of nine O 2*p*-derived bands which are hybridized with Ti or Hf *d* orbitals. The conduction band structure presents more pronounced differences because the Hf *d* states lie higher in energy and therefore hybridize with Sr *d* orbitals much more than those of Ti. The size of the indirect R-Γ gap is the most remarkable difference between the two band structures. These are 3.67 eV for $SrHfO_3$ and 1.84 eV for $SrTiO_3$. Blazey obtained by wavelength-modulation spectroscopy a gap of 3.34 eV for $SrTiO_3$ in the cubic phase,[16] which implies that our value is underestimated as is typical in LDA calculations for oxides. Another difference between the two band structures is that in $SrHfO_3$ the energy of the bands at -2 eV at Γ and at -0.78 eV at *M* are around 0.9 eV higher than the corresponding values in $SrTiO_3$. Hybridization between O *p* and B cation *d* bands can be observed looking at the sphere-projected density of states (DOS) shown in Fig. 2. The Ti *d* component of the DOS in the valence band region is greater than the Hf *d* component, and this implies that Ti 3*d*–O 2*p* covalency is more important than that of Hf 5*d*–O 2*p*. The magnitude of the sphere-projected DOS is, of course, somewhat dependent on the choice made for the R_i's. The question is then open whether the remarks made above about covalency remain true under changes in the sphere size radii. To check this point we calculate the sphere-projected DOS for $SrHfO_3$ for $R_{Hf}=2$ a.u. and integrate it in the valence band region to obtain the amount of Hf *d* charge. We obtain 0.66*e* in this case, 0.18*e* more than when $R_{Hf}=1.78$ is used, but still quite less than the 0.99*e* obtained for the *d* charge in the Ti sphere in $SrTiO_3$. We have checked, performing the calculation of the electronic structure of $SrTiO_3$ at the equilibrium volume

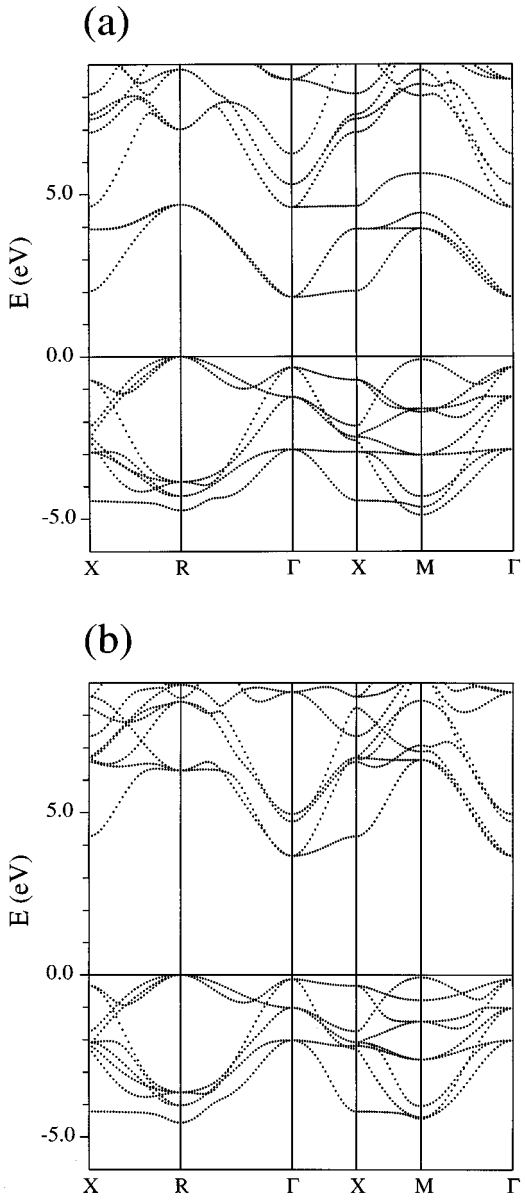

FIG. 1. Electronic band structure of $SrTiO_3$ (a) and $SrHfO_3$ (b) in the cubic perovskite structure at the calculated equilibrium volumes.

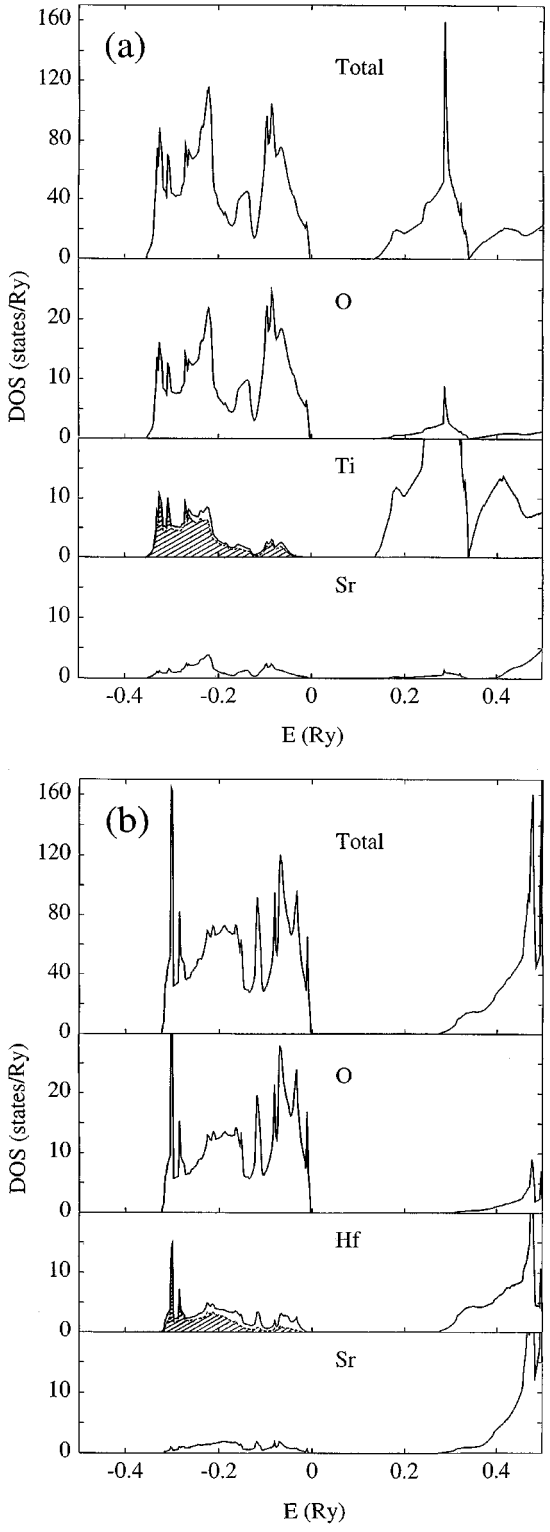

FIG. 2. Total electronic DOS and projections on the LAPW spheres for $SrTiO_3$ (a) and $SrHfO_3$ (b). The shadowed area indicates the *d* component contribution to the projected DOS of Ti or Hf in the valence band region. Energies are referred to the Fermi level.

of $SrHfO_3$, that the electronic-structure-related differences of both compounds mentioned in this paragraph are not due to the 5% greater lattice parameter of $SrHfO_3$. The effect of greater *B d*–O *p* covalency for Ti than for Hf as well as the larger gap obtained for $SrHfO_3$ than for $SrTiO_3$ may be attributed to the much smaller binding energy of *d* orbitals in Hf (8.14 eV) than in Ti (11.04 eV).[17] On the other hand, the larger Hf-5*d* orbital radius compared with that of Ti-3*d* would favor greater covalency in $SrHfO_3$. From our results it is evident that the effect of the binding energies is dominant. We would like to stress that our comparative analyses of the band structure of $SrTiO_3$ and $SrHfO_3$ shows the same relevant features than those made by Singh[8] for $KNbO_3$ and $KTaO_3$, although the differences found between the electronic structures of the Sr-based compounds are more pronounced.

To study the tendency of the $SrTiO_3$ and $SrHfO_3$ cubic perovskites to suffer a ferroelectric transition, we performed calculations of electronic properties of these systems for different displacements of the B ion in the 001 direction. In Fig. 3 we plot the total energy as a function of the B-ion displace-

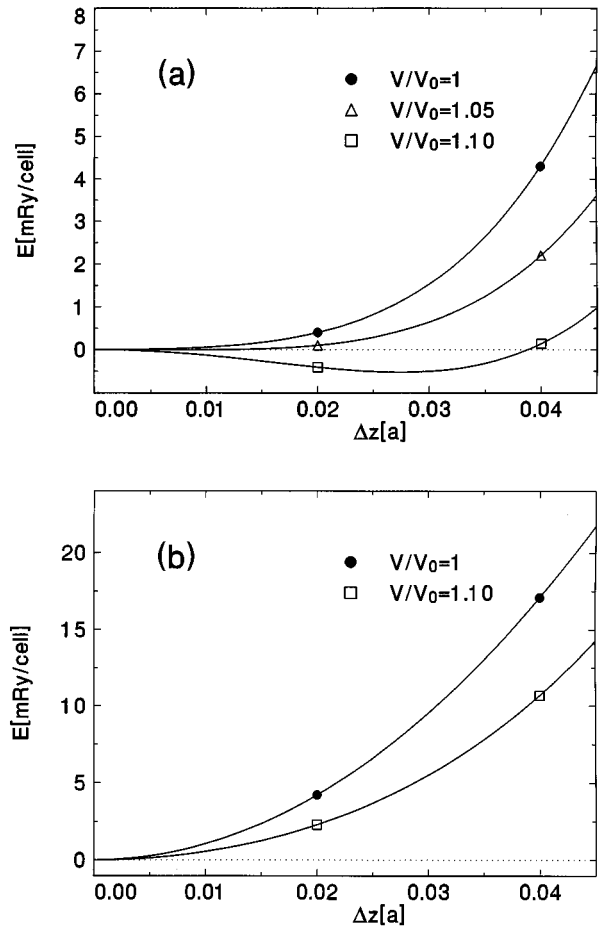

FIG. 3. Total energy of cubic $SrTiO_3$ (a) and $SrHfO_3$ (b) as a function of the displacement Δz of the B atom in the 001 direction for different volumes. Energies are referred to the undisplaced cases at the corresponding volumes. V_0 is the corresponding experimental equilibrium volume. The solid line shows the fourth-degree polynomial interpolation.

ment for different volumes. At the experimental equilibrium volume, neither of the two systems is energetically favored with the proposed ferroelectric transition, but energy differences with respect to the undisplaced ($\Delta z=0$) case are much smaller in the case of $SrTiO_3$. In fact when we repeat the calculation for a volume expansion greater than 5% (1.6% lattice constant increase), $SrTiO_3$ shows an instability and would undergo a ferroelectric transition. In particular, for a 10% volume expansion $SrTiO_3$ presents a shallow, but well-defined double well, while in $SrHfO_3$ the ferroelectric transition is still far away. We can then conclude from our calculations the existence of a tendency to ferroelectricity of cubic $SrTiO_3$ which is not present at all in the case of $SrHfO_3$. Our results for $SrTiO_3$ are in agreement with the present experimental and theoretical understanding that points out that $SrTiO_3$ is an incipient ferroelectric.[5,6] For $SrHfO_3$ there is much less work done, but the existing experimental results seem to show that no ferroelectric transition is favored in this system. Our electronic structure calculations for both $SrTiO_3$ and $SrHfO_3$ support the idea that the existence of a ferroelectric phase is to be associated to the degree of hybridization of the *B d* bands with O *p* bands.[9]

Once the B atom is separated from its cubic site, an electric field gradient (EFG) appears at its nuclear position and at that of Sr with principal axis in the 001 direction. In Table II we show the EFG as a function of the displacement Δz at the different atomic sites for two volumes. The behavior of the EFG is quite different at the O sites since these have noncubic symmetry and so a sizable EFG appears even when $\Delta z=0$. Also, at the O sites the EFG has a different sign in $SrTiO_3$ and $SrHfO_3$ when $\Delta z=0$ and varies strongly with volume. The EFG at the Hf site in $SrHfO_3$ has the same sign as at the Ti site in $SrTiO_3$, but the magnitude is almost 6 times larger and in both cases almost independent of volume. To understand the origin of the sign and magnitude of the EFG, it is usually useful to separate the contribution coming from inside the muffin-tin (MT) sphere of the atom under consideration and those arising from the rest of the lattice. In FPLAPW calculations, the contribution coming from the MT sphere may be expressed as

$$V_{zz}^{\mathrm{MT}}=-2\left(\frac{4\pi}{5}\right)^{1/2}\int_0^{R_{\mathrm{MT}}}\frac{\rho_{20}(r)r^2}{r^3}dr, \qquad (1)$$

where $\rho_{20}(r)$ is the $L=2$, $M=0$ radial component of the charge density when it is expanded in symmetrized spherical harmonics $Y_{LM}(\hat{\mathbf{r}})$ (Ref. 18) and it is assumed that the principal axis points in the *z* direction.

Let us now concentrate on the B-ion sites where we find that more than 93% of the contribution to the EFG comes from the interior of the B sphere. The origin of the sign of the EFG may be understood by looking at the charge asymmetries $\Delta n_p=1/2(n_{p_x}+n_{p_y})-n_{p_z}$ and $\Delta n_d=(n_{d_{xy}}+n_{d_{x^2-y^2}})-1/2(n_{d_{xz}}+n_{d_{yz}})-n_{d_{z^2}}$, where n_i is the charge of *i* character inside the MT sphere.[19] The valence charge inside the B sphere originates in the hybridization of valence orbitals of B atom with O-*p* orbitals. Displacing the B atom in the 001 direction increases hybridization of orbitals that have their charge pointing along the *z* direction, and so Δn_p and Δn_d (which are zero for $\Delta z=0$) become negative numbers and a negative contribution to the EFG is also obtained. The opposite holds for the contribution from semi-

TABLE II. Electric field gradients (in 10^{17} V/cm^2) at the different sites obtained when the B atom is desplaced from the center of the cube in the 001 direction at two volumes. The displacement Δz is given in units of the lattice parameter. V_0 is the corresponding experimental equilibrium volume. The principal axis points in the *z* direction except for the case of O(2) sites for which the principal axis points in the corresponding oxygen–B-atom direction.

		$V/V_0=1$			$V/V_0=1.1$		
	Δz	0.00	0.02	0.04	0.00	0.02	0.04
$SrTiO_3$	Sr	0.00	-0.14	-0.51	0.00	-0.13	-0.49
	Ti	0.00	-0.11	-0.71	0.00	-0.21	-0.80
	O(1)	0.17	-0.24	-1.29	1.21	0.80	-0.28
	O(2)	0.17	0.31	0.63	1.21	1.34	1.60
$SrHfO_3$	Sr	0.00	-0.10	-0.38	0.00	-0.09	-0.36
	Hf	0.00	-1.10	-3.97	0.00	-1.05	-3.80
	O(1)	-3.17	-3.49	-4.39	-1.72	-2.06	-3.00
	O(2)	-3.17	-3.03	-2.71	-1.72	-1.62	-1.36

core states because hybridization is associated with their depopulation and then a positive contribution to the EFG results. However, we obtained that the valence contribution is clearly dominant in these cases and then it determines the sign of the EFG. Concerning the different magnitude of the EFG in $SrTiO_3$ and $SrHfO_3$, it is clear that it is not related to the difference in the lattice parameters of the two systems since Table II shows little dependence of the EFG with volume. Then, to investigate this point, we looked at the contributions to $\rho_{20}(r)$ coming from the different orbital symmetries and, we obtain, as in Ref. 19, the p and d contributions to V_{zz}^{MT}. For the case $\Delta z=0.04$, we obtain for $V_{zz}^{\mathrm{MT}}(p)$ and $V_{zz}^{\mathrm{MT}}(d)$ the values of -0.29 and -0.48 for $SrTiO_3$ and -2.21 and -1.57 for $SrHfO_3$. This is an interesting result because looking at the d contribution, for example, one may think, in principle, that as Ti d–O p hybridization is greater than Hf d–O p hybridization the Ti atom would have to ''feel'' the asymmetry of the oxygen neighbors in $SrTiO_3$ more than the Hf in $SrHfO_3$. However, $V_{zz}^{\mathrm{MT}}(d)$ for Hf is 3 times $V_{zz}^{\mathrm{MT}}(d)$ for Ti. In fact, if we look at the charge asymmetry Δn_d, it is greater for the Ti in $SrTiO_3$ (-0.037) than for Hf in $SrHfO_3$ (-0.025). But even when the EFG is related to the charge asymmetries Δn_p and Δn_d, the factor $1/r^3$ in expression (1) strongly enhances the anisotropic contributions for very short distances. In the case of Hf the main contribution to integral (1) comes from $r\leqslant 0.1$ a.u., while in the case of Ti it is distributed up to $r=0.5$ a.u. This is related to the fact that Hf the 5d radial function has more weight near the origin than the Ti 3d nodeless radial function. This magnification of the charge asymmetry is even more drastic when comparing d to p contribution for the Hf site. Δn_p's for Hf valence and semicore states are less than 0.001 in both cases and, as we mentioned, they have different signs. However, $V_{zz}^{\mathrm{MT}}(p)>V_{zz}^{\mathrm{MT}}(d)$ for Hf in $SrHfO_3$.

Our calculated value of the EFG in $SrHfO_3$ for Δz between 0.02 and 0.04 in units of the lattice parameter is of the same order of magnitude as the measured value for the orthorhombic phase at the ^{181}Ta probe.[3] Although we find this agreement, we must remark that the experimentally observed orthorhombic distortion is quite different from the one we studied and that the experimental value is obtained at Ta. Still, the magnitudes of the Hf-O distance variations are of the same order in both cases.

SUMMARY AND CONCLUSIONS

Within the LDA we have analyzed the electronic structure of $SrHfO_3$ in the cubic phase with a direct comparison to $SrTiO_3$. We could identify the O p–B atom d hybridization as the main factor determining tendency to ferroelectricity. We find that $SrTiO_3$ has a pronounced facility to a ferroelectric instability, while $SrHfO_3$ has not. This is in agreement with the actual understanding of $SrTiO_3$ as an incipient ferroelectric and a nonobservation of ferroelectricity in the Hf compound. The detailed analysis of the EFG, which appears with the z-axis B-atom distortion, allows us to compare the microscopic interplay of p and d contributions in both compounds. The present study serves as a starting point for the study of the orthorhombic phase and its asociated EFG measured with PAC at the Ta- (Hf-) replaced site.

ACKNOWLEDGMENTS

We acknowledge the Consejo Nacional de Investigaciones Científicas y Técnicas (CONICET) for partial support of this work. One of us (G.F.) would like to aknowledge IFLYSIB for working facilities.

[1] A. Hoffman, Z. Phys. Chem. B **28**, 65 (1935).
[2] P. da R. Andrade, M. Forker, J.D. Rogers, and J.V. Kunzler, Phys. Rev. B **6**, 2560 (1972).
[3] S. Cuffini *et al.* (private communication).
[4] P. de la Presa, A. Ayala, and A. Lopez García (unpublished).
[5] K.A. Müller and H. Burkard, Phys. Rev. B **19**, 3593 (1979); R. Viana, P. Lunkenheimer, J. Hemberger, R. Böhmer, and A. Loidl, *ibid.* **50**, 601 (1994).
[6] W. Zhong and D. Vanderbilt, Phys. Rev. Lett. **74**, 2587 (1995); Phys. Rev. B **53**, 5047 (1996).
[7] C. Lasota, Ch. Wang, R. Yu, and H. Krakauer, Bull. Am. Phys. Soc. **41**, 309 (1996).
[8] D. Singh, Phys. Rev. B **53**, 176 (1996).
[9] R.E. Cohen and H. Krakauer, Phys. Rev. B **42**, 6416 (1990).
[10] O.K. Andersen, Phys. Rev. B **12**, 3060 (1975); S.H. Wei and H. Krakauer, Phys. Rev. Lett. **55**, 1200 (1985).
[11] P. Blaha, K. Schwarz, P. Dufek, and R. Augustyn, computer code WIEN95, Technical University of Vienna, 1995 [improved and updated UNIX version of the original copyrighted WIEN code, which was published by P. Blaha, K. Schwarz, P. Sorantin, and S.B. Trickey, Comput. Phys. Commun. **59**, 399 (1990)].
[12] D. Singh, Phys. Rev. B **43**, 6388 (1991).
[13] L. Hedin and B.I. Lundqvist, J. Phys C **4**, 2064 (1971).
[14] T. Mitsui *et al.*, in *Ferro- and Antiferroelectric Substances*, edited by K.-H. Hellwege and A. M. Hellwege, Landolt-Börnstein, New Series, Group III, Vol. 3 (Springer-Verlag, Berlin, 1969).
[15] R.D. King-Smith and D. Vanderbilt, Phys. Rev. B **49**, 5828 (1994).
[16] K. W. Blazey, Phys. Rev. Lett. **27**, 146 (1971).
[17] W.A. Harrison, *Electronic Structure and the Properties of Solids* (Freemann, San Francisco, 1980).
[18] K. Schwartz, C. Ambrosch-Draxl, and P. Blaha, Phys. Rev. B **42**, 2051 (1990).
[19] P. Blaha, K. Schwartz, and P.H. Dederichs, Phys. Rev. B **37**, 2792 (1988).